Volume 21
Number 25
7 July 2023
Pages 5131-5306

Organic & Biomolecular Chemistry

rsc.li/obc

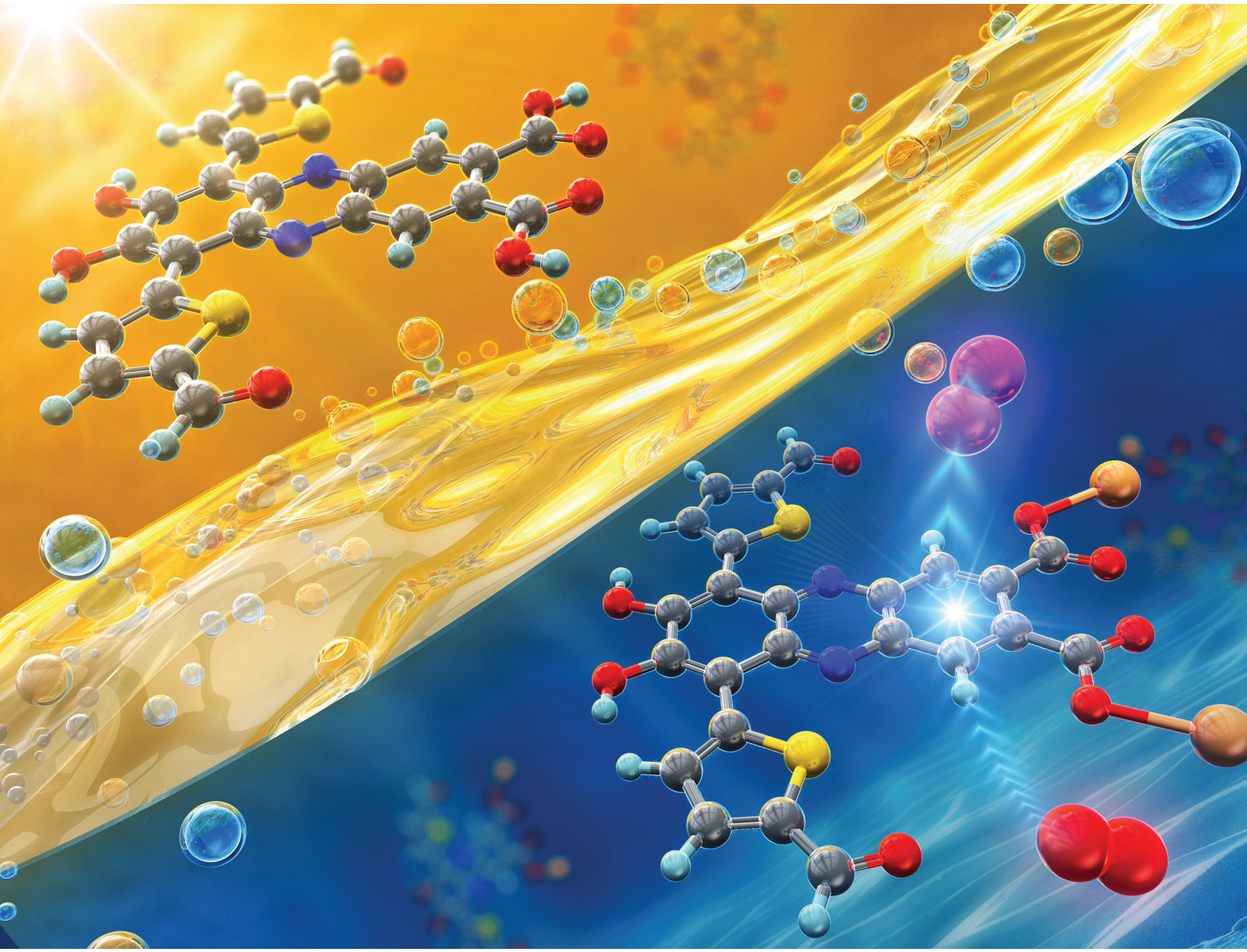

ISSN 1477-0520

ROYAL SOCIETY OF CHEMISTRY

PAPER

Yousuke Ooyama *et al.*

Development of water-soluble phenazine-2,3-diol-based photosensitizers for singlet oxygen generation

Organic & Biomolecular Chemistry

ROYAL SOCIETY OF CHEMISTRY

PAPER

View Article Online
View Journal | View Issue

Cite this: *Org. Biomol. Chem.*, 2023, **21**, 5194

Development of water-soluble phenazine-2,3-diol-based photosensitizers for singlet oxygen generation†

Kazunori Yagi, Kazuki Ohira, Keita Yamana, Keiichi Imato, Riku Kawasaki, Atsushi Ikeda and Yousuke Ooyama *

Received 31st March 2023,
Accepted 4th May 2023

DOI: 10.1039/d3ob00491k

rsc.li/obc

Phenazine-2,3-diol-based dyes, **KY-1Na** and **KY-2Na** bearing one and two carboxylic acid sodium salts, respectively, have been newly developed as water-soluble photosensitizers (PSs) possessing the ability to generate singlet oxygen ($^1O_2$). In order to evaluate the solubility of **KY-1Na** and **KY-2Na** in water, the hydrophobicity/hydrophilicity of the two PSs was investigated by experimental measurement of the logarithms (log $P_{o/w}$) of the 1-octanol/water partition coefficient ($P_{o/w}$) for the PS. The log $P_{o/w}$ values of both **KY-1Na** and **KY-2Na** were determined to be −0.9, indicating that both the PSs are more hydrophilic than Rose Bengal (−0.6) and have hydrophilicity equivalent to methylene blue (−0.9). Both the PSs in water show a broad photoabsorption band in the range of 500 to 600 nm. Thus, we estimated the $^1O_2$ quantum yields (Φ_Δ) of **KY-1Na** and **KY-2Na** in water by using 9,10-anthracenediyl-bis(methylene)dimalonic acid (ABDA) as a water-soluble $^1O_2$ scavenger. It was found that in water the Φ_Δ value (0.19) of **KY-2Na** is higher than that of **KY-1Na** (0.06). Density functional theory (DFT) calculations suggested that the highest occupied molecular orbital (HOMO) and lowest unoccupied molecular orbital (LUMO) distributions for the molecular structure of **KY-2Na** are adequately separated, leading to a decrease in the energy gap (ΔE_{ST}) between the singlet state (S_1) and the triplet state (T_1) that causes efficient intersystem crossing (ISC), compared to that for the molecular structure of **KY-1Na**. Indeed, time-dependent DFT (TD-DFT) calculations demonstrated that the $\Delta E_{ST}(S_1–T_1)$ value (0.82 eV) of **KY-2Na** is smaller than that (0.98 eV) of **KY-1Na**, resulting in a relatively high Φ_Δ value of **KY-2Na**. Consequently, we demonstrate that phenazine-2,3-diol-based PSs bearing carboxylic acid salts possess high solubility and moderate $^1O_2$ generation ability in water.

Introduction

Singlet oxygen ($^1O_2$) generated by light irradiation to photosensitizers (PSs),[1] which is one of the reactive oxygen species (ROS), has gained more and more attention as an effective and convenient oxidant of alkenes and dienes for Schenck–ene reactions and [2 + 2]- and [4 + 2]-cycloadditions in organic synthesis,[2–5] degradation of water pollutants in environmental and quality control monitoring systems,[6] inactivation of microbiological contamination in point-of-use water disinfection systems,[7] and cancer treatment in photodynamic therapy (PDT).[8] $^1O_2$ is generally produced through the following processes: initially, the PS (^{1}PS) absorbs light ($h\nu$) to generate the singlet excited state (^{1}PS*), and then the ^{1}PS* undergoes intersystem crossing (ISC) to generate the triplet excited state (^{3}PS*). Subsequent energy transfer from the photoexcited PS (^{3}PS*) to triplet oxygen ($^3O_2$) produces $^1O_2$. Thus, in order to obtain a high $^1O_2$ quantum yield (Φ_Δ), it is necessary to enhance the ISC efficiency of PSs. Moreover, for use in water purification systems and PDT, the PSs are required to possess high solubility in water as well as efficient ISC. Methylene blue (**MB**),[9] Rose Bengal (**RB**),[10] and hydrophobically modified porphyrin derivatives[11] have been used as water-soluble PSs with high $^1O_2$ Φ_Δ values (0.50–0.60 for **MB**,[9b,c] 0.70–0.80 for **RB**,[9b,10b] and 0.50–0.60 for free base 5,10,15,20-tetrakis(4-carboxylatophenyl)porphyrin,[11a,b] respectively). Meanwhile, halogen atoms such as iodide and bromide atoms are often introduced into chromophores (*e.g.* **RB**) to promote ISC based on spin–orbit coupling,[11] but they cause dark cytotoxicity.[12] Indeed, **MB** as a halogen atom-free-heteroanthracene-based PS[13] is used as not only a reference water-soluble PS for the evaluation of Φ_Δ,[9b,c] but also a fungicide and antidote in aquaculture.[9f,g]

Thus, in our previous work, we have designed and developed phenazine-2,3-diol-based dyes (**KO-0-3**)[14] as halogen

Applied Chemistry Program, Graduate School of Advanced Science and Engineering, Hiroshima University, 1-4-1 Kagamiyama, Higashi-Hiroshima 739-8527, Japan. E-mail: yooyama@hiroshima-u.ac.jp

† Electronic supplementary information (ESI) available. See DOI: https://doi.org/10.1039/d3ob00491k

atom-free-heteroanthracene-based PSs and demonstrated that the modification of the phenazine-2,3-diol chromophore with formyl groups promotes ISC, leading to efficient $^1O_2$ generation (Fig. 1a). According to the El-Sayed rule, formyl and carbonyl substituents in a chromophore skeleton facilitate the ISC from the singlet (S_n) to triplet (T_n) states, that is, by the change in the molecular orbital type such as transitions of $^1(n\pi^*)$ to $^3(\pi\pi^*)$ and $^1(\pi\pi^*)$ to $^3(n\pi^*)$. In fact, **KO-1-3** exhibited moderate $^1O_2$ generation ability (Φ_Δ = 0.22–0.41) in THF.

In this work, in order to attain the solubility of phenazine-2,3-diol-based PSs in water, we have developed **KY-1Na** and **KY-2Na** bearing one and two carboxylic acid sodium salts, respectively, as the water-soluble derivatives of **KO-2** exhibiting a moderate Φ_Δ value (0.17) in DMSO (Fig. 1b). Actually, in order to evaluate the solubility of **KY-1Na** and **KY-2Na** in water, the hydrophobicity/hydrophilicity of the two PSs was investigated by experimental measurement of the logarithms ($\log P_{o/w}$) of the 1-octanol/water partition coefficient ($P_{o/w}$) for the PS. Both the PSs in water show a broad photoabsorption band in the range of 500 to 600 nm. It was found that in water **KY-2Na** exhibits a moderate Φ_Δ value, which is higher than that of **KY-1Na**. Density functional theory (DFT) and time-dependent DFT (TD-DFT) calculations were performed to gain insight into the $^1O_2$ generation properties of **KY-1Na** and **KY-2Na** based on the ISC efficiency. Herein we report that the introduction of carboxylic acid salts into the phenazine-2,3-diol chromophore is effective in yielding solubility in water and a small energy gap (ΔE_{ST}) between the S_1 state and the T_1 state for efficient ISC, leading to the development of water-soluble halogen-atom-free-heteroanthracene-based PSs.

Results and discussion

Synthesis

Phenazine-2,3-diol-based PSs, **KY-1** and **KY-2** bearing one and two carboxylic acids, respectively, and their sodium salt derivatives **KY-1Na** and **KY-2Na**, were synthesized by a stepwise synthetic protocol (Scheme 1). We prepared compounds **1** and **2**,[15] respectively, for the construction of the phenazine skeleton and the introduction of the formylthiophene unit on the chromophore by the Stille coupling (see the ESI†). Phenazine-2,3-diol chromophores **3** and **4** were prepared by the cyclodehydration of 2,5-dibromo-3,6-dihydroxy-*p*-quinone with methyl 3,4-diaminobenzoate or compound **1**, respectively, and then converted into methoxymethyl (MOM)-protected compounds **5** and **6**, respectively. The Stille coupling reaction of **5** or **6** with compound **2** gave compounds **7** and **8**, respectively. Compounds **7** and **8** were hydrolyzed by treatment with a base to generate compounds **9** and **10**, respectively, and then the hydrolysis of **9** and **10** with an acid gave the carboxylic acids **KY-1** and **KY-2**, respectively. Finally, **KY-1Na** and **KY-2Na** were obtained by treatment of **KY-1** and **KY-2**, respectively, with a base.

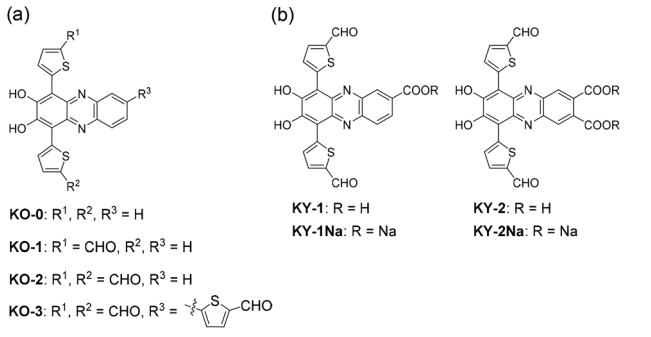

Fig. 1 Chemical structures of phenazine-2,3-diol-based PSs, (a) **KO-0-3** in our previous study and (b) **KY-1**, **KY-2**, **KY-1Na**, and **KY-2Na** in this study.

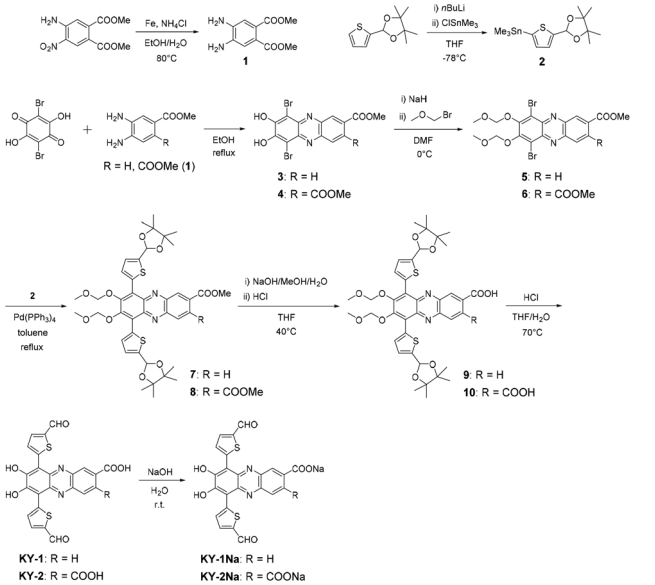

Scheme 1 Synthetic route to phenazine-2,3-diol-based PSs **KY-1**, **KY-2**, **KY-1Na**, and **KY-2Na**.

In order to evaluate the hydrophobicity/hydrophilicity of **KY-1Na** and **KY-2Na**, the logarithms ($\log P_{o/w}$)[16] of the 1-octanol/water partition coefficient ($P_{o/w}$) for the PS were measured experimentally. The $\log P_{o/w}$ values of both **KY-1Na** and **KY-2Na** were determined to be −0.9, indicating that both the PSs are more hydrophilic than **RB** (−0.6)[10c] and have hydrophilicity equivalent to **MB** (−0.9).[9d,e] Incidentally, **KO-2** exhibits hydrophobicity with a $\log P_{o/w}$ value of 1.3. Thus, this fact indicates that **KY-1Na** and **KY-2Na** possess high solubility in water.

Optical properties

The photoabsorption and fluorescence spectra of **KY-1Na** and **KY-2Na** in DMSO and in water (D_2O) are shown in Fig. 2 with those of **KO-2**, **KY-1**, and **KY-2** in DMSO as references for the characterization of the photoabsorption properties of **KY-1Na** and **KY-2Na**, and their optical data are summarized in Table 1. All the five dyes show an intense photoabsorption maximum (λ_{max}^{abs}) at around 400–450 nm with a relatively high molar extinction coefficient (ε_{max} = 25 000–30 000 M^{-1} cm^{-1}), which

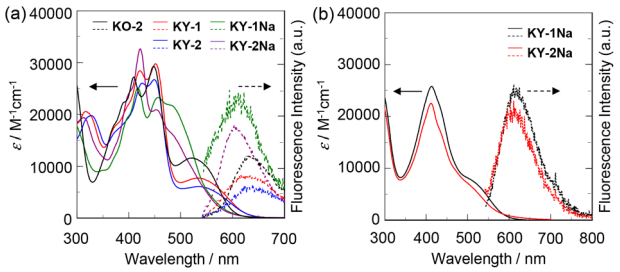

Fig. 2 (a) Photoabsorption and fluorescence spectra (λ^{ex} = 532 nm) of **KO-2**, **KY-1**, **KY-2**, **KY-1Na**, and **KY-2Na** (5.0 × 10^{-5} M) in DMSO. (b) Photoabsorption and fluorescence spectra (λ^{ex} = 532 nm) of **KY-1Na** and **KY-2Na** (5.0 × 10^{-5} M) in D_2O.

Table 1 Optical data and $^1O_2$ quantum yields (Φ_Δ) of **KO-2**, **KY-1**, **KY-2**, **KY-1Na** and **KY-2Na**

Dye	λ^{abs}_{max}/nm (ε_{max}/M^{-1} cm^{-1})	ε/M^{-1} cm^{-1} @λ^{abs} = 532 nm	λ^{fl}_{max}/nm (Φ_{fl})[c]	Φ_Δ
KO-2	522 (11 500)[a]	11 300[a]	634 (0.03)[a]	0.17[d]
KY-1	534 (7700)[a]	7700[a]	625 (<0.02)[a]	0.14[d]
KY-2	534 (6000)[a]	6000[a]	631 (<0.02)[a]	0.17[d]
KY-1Na	486[shoulder] (21 500)[a]	9600[a]	611 (0.02)[a]	0.13[d]
KY-2Na	486[shoulder] (15 900)[a]	7700[a]	603 (0.02)[a]	0.32[d]
KY-1Na	500[shoulder] (8100)[b]	6100[b]	611 (<0.02)[b]	0.06[e]
KY-2Na	500[shoulder] (7100)[b]	4500[b]	611 (<0.02)[b]	0.19[e]

[a] In DMSO. [b] In D_2O. [c] Fluorescence quantum yields (Φ_{fl}) were determined using a calibrated integrating sphere system (λ^{ex} = 532 nm). [d] $^1O_2$ quantum yields (Φ_Δ) based on the relative decomposition rate of DPBF using **RB** as the standard PS (Φ_Δ = 0.76 in DMSO,[9a] see Fig. S44a†) and DPBF as the $^1O_2$ scavenger under irradiation with monochromatic light (532 nm, 300 μW cm^{-2}) in DMSO. [e] Φ_Δ based on the relative decomposition rate of AMDA using **RB** as the standard PS (Φ_Δ = 0.75 in water,[9b] see Fig. S44b†) and AMDA as the $^1O_2$ scavenger under irradiation with monochromatic light (532 nm, 300 μW cm^{-2}) in D_2O/DMSO (99 : 1, v/v).

can be assigned to the π → π* transition of the phenazine skeleton containing two formylthiophene units.[14] In addition, for **KO-2**, **KY-1**, and **KY-2**, a broad photoabsorption band (λ^{abs}_{max} = 520–535 nm) with a moderate ε_{max} value (6000–12 000) was also observed in the range of 500 to 650 nm, which is ascribable to the formation of phenoxide ions by the partial deprotonation of the hydroxyl groups.[14] On the other hand, for **KY-1Na** and **KY-2Na** both in DMSO and in water, the photoabsorption spectra in the range of 500 to 600 nm are significantly broadened, and exhibit a hypsochromic shift and become a shoulder band, compared to those of **KO-2**, **KY-1**, and **KY-2** in DMSO. This fact indicates that **KY-1Na** and **KY-2Na** existed as carboxylate anion (–COO^-) species in DMSO as well as in water.[17] In the corresponding fluorescence spectra, all the five dyes show a feeble fluorescence band with a fluorescence maximum wavelength (λ^{fl}_{max}) at 600–635 nm. In fact, their fluorescence quantum yields (Φ_{fl}) were significantly low (≤0.03).

$^1O_2$ generation

We evaluated the $^1O_2$ generation ability of the phenazine-2,3-diol-based PSs **KO-2**, **KY-1**, **KY-2**, **KY-1Na**, and **KY-2Na** by using an $^1O_2$ scavenger. It is well known that 1,3-diphenylisobenzofuran (DPBF) acts as an efficient $^1O_2$ scavenger in organic solvents to produce its oxidized product, *o*-dibenzoylbenzene.[18a,b] Meanwhile, 9,10-anthracenediyl-bis(methylene)dimalonic acid (ABDA), which can react rapidly and irreversibly with $^1O_2$ to produce the corresponding endoperoxide (endoperoxideABDA), is widely used as a water-soluble $^1O_2$ scavenger.[18b,c] Therefore, $^1O_2$ generation by the five PSs was investigated by monitoring the changes in the photoabsorption spectra of DPBF in the DMSO solution of each PS and ABDA in the aqueous solution (D_2O/DMSO 99 : 1, v/v) of **KY-1Na** and **KY-2Na** under photoirradiation (Fig. 3a–d for **KY-1Na** and **KY-2Na**, and Fig. S45† for **KO-2**, **KY-1**, **KY-2**, and **RB** in DMSO). DMSO and D_2O/DMSO were bubbled with air

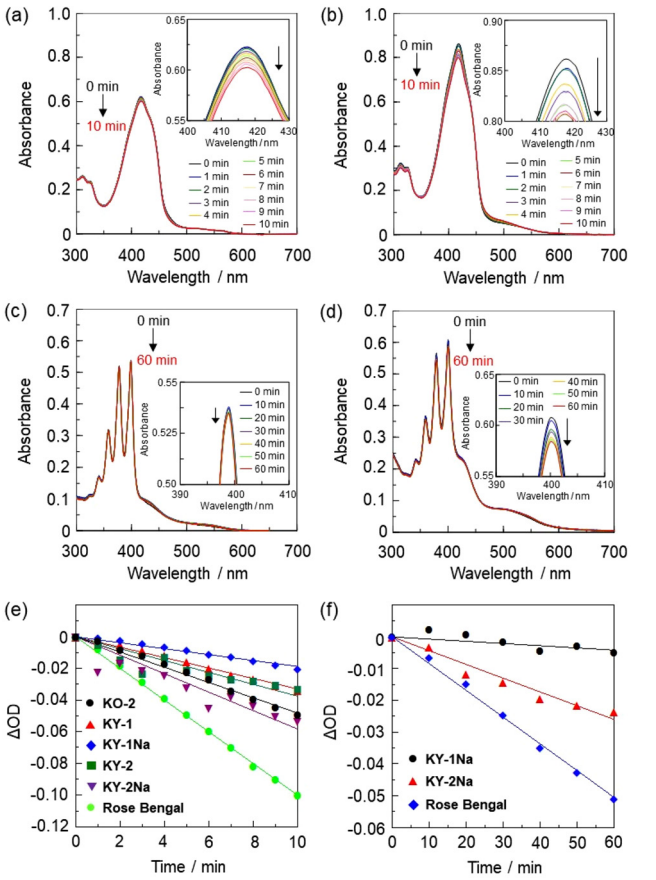

Fig. 3 Photoabsorption spectra for the photooxidation of DPBF (5.0 × 10^{-5} M) in the presence of (a) **KY-1Na** and (b) **KY-2Na** under photoirradiation with 532 nm (300 μW cm^{-2}) in DMSO. Insets are magnifications of maxima in the spectra at around 415 nm. Photoabsorption spectra for the photooxidation of ABDA (5.0 × 10^{-5} M) in the presence of (c) **KY-1Na** and (d) **KY-2Na** under photoirradiation with 532 nm (300 μW cm^{-2}) in D_2O/DMSO (99 : 1, v/v). Insets are magnifications of maxima in the spectra at around 400 nm. (e) Plots of ΔOD at around 415 nm for the photooxidation of DPBF in the presence of **KO-2**, **KY-1**, **KY-2**, **KY-1Na**, **KY-2Na**, and **RB** against the photoirradiation time (532 nm, 300 μW cm^{-2}) in DMSO. (f) Plots of ΔOD at around 400 nm for the photooxidation of ABDA in the presence of **KY-1Na**, **KY-2Na**, and **RB** against the photoirradiation time (532 nm, 300 μW cm^{-2}) in D_2O/DMSO (99 : 1, v/v).

for 15 min prior to preparing solutions. Air-saturated DMSO solutions containing DPBF or aqueous solutions containing ABDA and each PS were irradiated with monochromatic light at 532 nm (300 μW cm^{-2}) that was obtained by the passage of a xenon light source through a monochromator. In all the DMSO solutions, the photoabsorption of DPBF at around 415 nm decreased with the increase in the photoirradiation time (Fig. 3a, b and S45†), which indicates that DPBF reacted with $^1O_2$ generated by the photosensitization of the PSs. In order to make clear the difference in $^1O_2$ generation ability between the five PSs, the changes in the optical density (ΔOD) at around 415 nm of DPBF are plotted against the photoirradiation time (Fig. 3e), and the slope (m_{sam}) is used to estimate the $^1O_2$ quantum yield (Φ_Δ): the Φ_Δ values for PSs were determined by the relative method using the slope value (m_{ref} = −0.0100) of the plot for **RB** (Φ_Δ = 0.76 in DMSO)[9a] as a standard (Table 1). Indeed, the correlation coefficient (R^2) values for the calibration curves of the five PSs are 0.860–0.996, which indicates good linearity, and the m_{sam} values become steeper in the following order: **KY-1Na** (−0.0018) < **KY-1** (−0.0033) ≈ **KY-2** (−0.0037) < **KO-2** (−0.0048) < **KY-2Na** (−0.0058). It was found that the Φ_Δ values (0.13–0.17) of **KY-1**, **KY-2**, and **KY-1Na** are equivalent to that of **KO-2** (Φ_Δ = 0.17), and surprisingly **KY-2Na** exhibited the highest $^1O_2$ generation ability (Φ_Δ = 0.32). Moreover, for the aqueous solutions of **KY-1Na** and **KY-2Na**, the photoabsorption of ABDA at around 400 nm decreased with the increase in the photoirradiation time (Fig. 3c and d), indicating ABDA reacted with $^1O_2$ generated by the photosensitization of the PSs. The plots of ΔOD at around 400 nm of ABDA *versus* the photoirradiation time revealed that the calibration curve for **KY-2Na** shows good linearity with an R^2 value of 0.956, but that for **KY-1Na** has a mediocre R^2 value (0.756) which may be due to a small change in the ΔOD (Fig. 3f). In fact, the m_{sam} value (−0.00043) for **KY-2Na** is larger than that (−0.00007) for **KY-1Na**. Thus, the Φ_Δ values for PSs were determined by the relative method using the slope value (m_{ref} = −0.00084) of the plot for **RB** (Φ_Δ = 0.75 in water)[9b] as a standard. It is worth noting here that in water the Φ_Δ value (0.19) of **KY-2Na** is much higher than that of **KY-1Na** (0.06), indicating that **KY-2Na** bearing two carboxylic acid sodium salts is superior to **KY-1Na** bearing one carboxylic acid sodium salt for $^1O_2$ generation. Meanwhile, both the Φ_{fl} and Φ_Δ values for phenazine-2,3-diol-based photosensitizers are quite low which indicates a large loss of the excited energy. Thus, we performed time-resolved fluorescence spectroscopy to determine the fluorescence lifetime (τ_{fl}), radiative rate constant ($k_r = \Phi_{fl}/\tau_{fl}$), and nonradiative rate constant ($k_{nr} = (1 - \Phi_{fl})/\tau_{fl}$) for **KY-2Na** in DMSO. The τ_{fl}, k_r, and k_{nr} values for **KY-2Na** are 2.17 ns, 9.20×10^6 s^{-1}, and 4.51×10^8 s^{-1}, respectively. The ratio of the nonradiative constant to radiative constant (k_{nr}/k_r) is estimated to be 49, indicating that the k_{nr} value is significantly larger than the k_r value. Thus, this result suggests that for the phenazine-2,3-diol-based photosensitizers, the accelerated nonradiative decay of the excited state may be the main reason for the large loss of the excited energy. Nevertheless, the photodynamic activities of **KY-1Na** and **KY-2Na** for PDT in murine colon carcinoma cells (Colon26)[19] under visible light irradiation (>510 nm) were investigated. Colon26 cells were incubated with **KY-1Na** or **KY-2Na** for 24 h. The cells were irradiated for 30 min (9 mW), and cell viability was determined after 24 h of incubation using a WST-8 assay. Both under dark and irradiation conditions, unfortunately, the cell viability changed little despite the increasing concentration of **KY-1Na** and **KY-2Na** (Fig. S46†). In order to investigate the degree of cellular uptake of **KY-2Na** in Colon26 cells, we performed confocal laser scanning microscopy (CLSM) for live cell fluorescence imaging. As is expected, the fluorescence image originating from the photosensitizer **KY-2Na** was not observed (Fig. S47†). These low photodynamic activities indicate that **KY-1Na** and **KY-2Na** with high solubility in water ($\log P_{o/w}$ = −0.9) are impermeable to the cell membrane of Colon26.[20] Consequently, these results suggested that the $^1O_2$ generation ability of phenazine-2,3-diol-based PSs is attributed to the facilitated ISC from the singlet to triplet states by the carbonyl groups based on El-Sayed's rule which allows the change in the molecular orbital type such as transitions of $^1(n\pi^*)$ to $^3(\pi\pi^*)$ and $^1(\pi\pi^*)$ to $^3(n\pi^*)$. Moreover, it was found that **KY-2Na** possesses moderate $^1O_2$ generation ability not only in DMSO but also in water, which is attributed to the efficient ISC characteristics, as discussed later in the next section.

Theoretical calculations

Density functional theory (DFT) and time-dependent DFT (TD-DFT) calculations[21] at the B3LYP/6-311G(d,p)/DMSO-IEFPCM level for **KO-2**, **KY-1**, and **KY-2**, the B3LYP/6-311+G(d,p)/DMSO-IEFPCM level for **KY-1Na** and **KY-2Na** in carboxylate anion forms, and the B3LYP/6-311+G(d,p)/Water-IEFPCM level for **KY-1Na** and **KY-2Na** in carboxylate anion forms were performed to gain insight into the $^1O_2$ generation properties of these PSs based on the ISC efficiency (Fig. 4). There is little difference in the highest occupied molecular orbital (HOMO) and the lowest unoccupied molecular orbital (LUMO) energy levels among the five PSs. Moreover, the DFT calculations indicate that for **KO-2**, **KY-1**, **KY-2**, and **KY-1Na**, the HOMOs are delocalized over the phenazine-2,3-diol skeleton and formylthiophene units. On the other hand, for **KY-2Na**, the HOMO is delocalized on the phenazine-2,3-diol skeleton containing the carboxylate anion. Meanwhile, the LUMOs for **KO-2**, **KY-1Na**, and **KY-2Na** are delocalized over the phenazine-2,3-diol skeleton and formylthiophene units, but those for **KY-1** and **KY-2** are delocalized mainly on the phenazine-2,3-diol skeleton and localized partially on formylthiophene units. Thus, DFT calculations suggested that the HOMO and LUMO distributions for the molecular structure of **KY-2Na** are adequately separated, leading to a decrease in the energy gap (ΔE_{ST}) between the S_1 state and the T_1 state that causes efficient ISC,[22,23] compared to that for the molecular structures of **KO-2**, **KY-1**, **KY-2**, and **KY-1Na**. Indeed, the TD-DFT calculations demonstrated that the ΔE_{ST} (S_1–T_1) values (0.80 eV in DMSO and 0.82 eV in water) of **KY-2Na** are smaller than those (0.96 eV in DMSO and 0.98 eV in water) of **KY-1Na**, that (0.85 eV) of **KY-1** and that of (0.81 eV) of **KY-2** as well as that (0.93

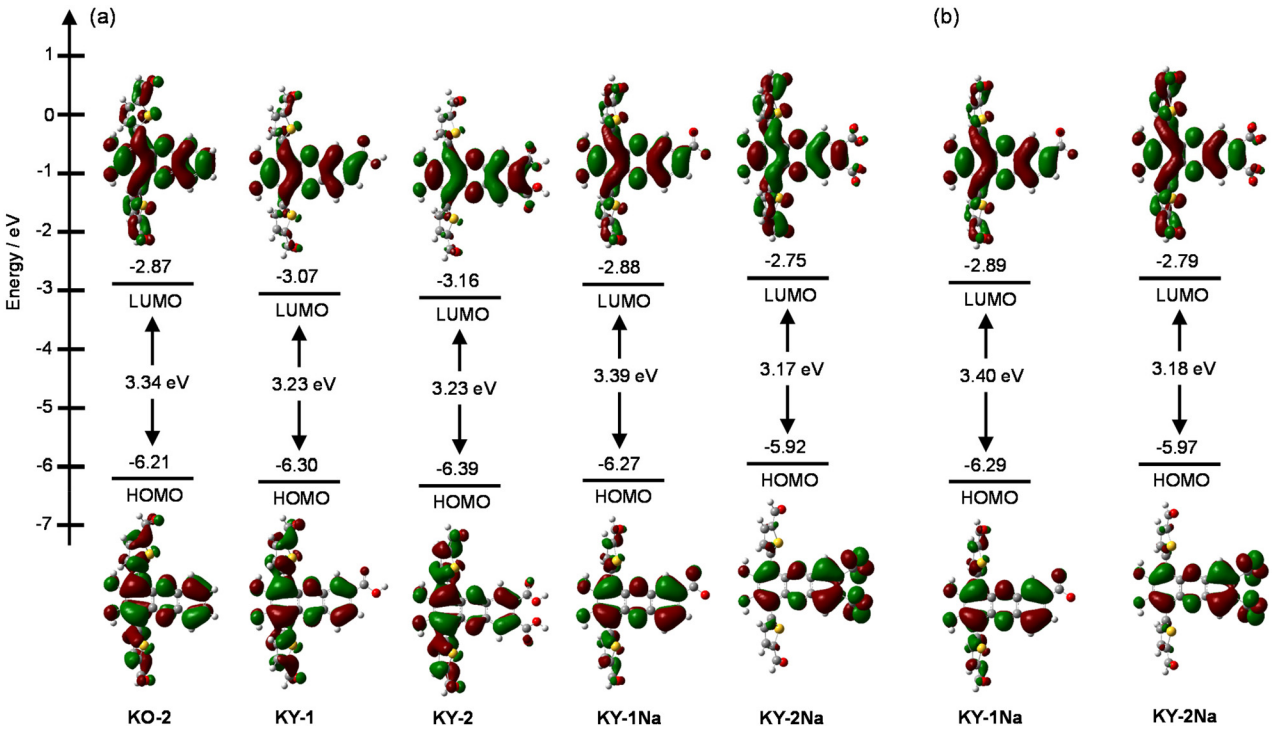

Fig. 4 Energy level diagram, HOMO, and LUMO of (a) **KO-2**, **KY-1**, and **KY-2** at the B3LYP/6-311G(d,p)/DMSO-IEFPCM level, **KY-1Na** and **KY-2Na** as carboxylate anions at the B3LYP/6-311+G(d,p)/DMSO-IEFPCM level, and (b) **KY-1Na** and **KY-2Na** at the B3LYP/6-311+G(d,p)/Water-IEFPCM level using DFT calculations.

eV) of **KO-2**, resulting in a relatively high Φ_Δ value of **KY-2Na** (Table S7, ESI†). Consequently, we demonstrated that phenazine-2,3-diol chromophore-bearing carboxylic acid salts can act as water-soluble halogen-atom-free-heteroanthracene-based PSs for $^1O_2$ generation.

Conclusions

We have designed and developed phenazine-2,3-diol-based dyes, **KY-1Na** and **KY-2Na** bearing one and two carboxylic acid sodium salts, respectively, as water-soluble halogen-atom-free-heteroanthracene-based photosensitizers (PSs) possessing the ability to generate $^1O_2$. The logarithms ($\log P_{o/w}$) of the 1-octanol/water partition coefficient ($P_{o/w}$) demonstrated that both **KY-1Na** and **KY-2Na** are more hydrophilic than Rose Bengal and have hydrophilicity equivalent to methylene blue. Both the PSs in water show a broad photoabsorption band in the range from 500 to 600 nm. It was found that in water **KY-2Na** exhibits a moderate $^1O_2$ quantum yield (Φ_Δ = 0.19) value, which is higher than that (0.06) of **KY-1Na**. Density functional theory (DFT) calculations suggested that the HOMO and LUMO distributions for the molecular structure of **KY-2Na** are adequately separated, leading to a decrease in the energy gap (ΔE_{ST}) between the S_1 state and the T_1 state that causes efficient intersystem crossing (ISC), compared to that for the molecular structure of **KY-1Na**. Indeed, time-dependent DFT (TD-DFT) calculations demonstrated that the ΔE_{ST} (S_1–T_1) value (0.82 eV) of **KY-2Na** is smaller than that (0.98 eV) of **KY-1Na**, resulting in a relatively high Φ_Δ value of **KY-2Na**. Consequently, we propose that phenazine-2,3-diol chromophore-bearing carboxylic acid salts are one of the promising water-soluble halogen-atom-free-heteroanthracene-based PSs for $^1O_2$ generation. Further studies on adjustment in the hydrophobicity/hydrophilicity of phenazine-2,3-diol-based PSs suitable for the light-induced cytotoxicity assessment are now in progress to gain insight into the $^1O_2$ generation under physiological conditions.

Experimental

General

All solvents and reagents were used as received unless otherwise noted. Rose Bengal (**RB**) was purchased from Sigma Aldrich and recrystallized from methanol twice for the use in the photoabsorption spectral measurement. 1,3-Diphenylisobenzofuran (DPBF) was purchased from Tokyo Chemical Industry and recrystallized from a mixture of dichloromethane and methanol for use in the photoabsorption spectral measurement. High-grade 9,10-anthracenediyl-bis(methylene)dimalonic acid (ABDA) was purchased from Funakoshi Co., Ltd. ^1H NMR and ^{13}C NMR spectra were recorded using a Varian-500 (500 MHz) FT NMR spectrometer. FT-IR spectra were recorded using a Shimadzu IRTracer-100 instrument. High-resolution mass spectral data were acquired

using a Thermo Fisher Scientific LTQ Orbitrap XL mass spectrometer. Photoabsorption spectra were recorded using Shimadzu and UV-3600-plus spectrophotometers. Fluorescence spectra were measured using a Hitachi F-4500 spectrophotometer. The fluorescence quantum yields (Φ_{fl}) were determined with a Hamamatsu C9920-01 instrument equipped with a CCD using a calibrated integrating sphere system. Fluorescence decay measurement was performed on a HORIBA DeltaFlex modular fluorescence lifetime system, using a Nano LED pulsed diode excitation source (451 nm). The irradiance of monochromatic and continuous light for photosensitizing reactions was adjusted using a Newport 1918-C optical power meter.

Synthesis

Methyl 6,9-dibromo-7,8-dihydroxyphenazine-2-carboxylate (3). A solution of bromanilic acid (2.98 g, 10.0 mmol) and methyl 3,4-diaminobenzoate (1.66 g, 10.0 mmol) in ethanol (500 mL) was stirred at 80 °C overnight. After the disappearance of the reactants, the reaction mixture was cooled to room temperature, and the precipitate was filtered and washed with a small amount of ethanol to obtain **3** as a red solid (3.80 g, 89% yield); m.p. over 300 °C; IR (ATR): $\tilde{\nu}$ = 3204, 2957, 1709, 1624, 1609, 1572, 1551 cm^{-1}; ^1H NMR (500 MHz, DMSO-d_6): δ = 8.61 (br, 1H, aromatic), 8.20 (d, J = 8.60 Hz, 1H, aromatic), 8.12 (d, J = 8.70 Hz, 1H, aromatic) ppm; the ^{13}C NMR spectrum could not be obtained because of the low solubility in any solvents; HRMS (APCI): m/z found 424.87924 $[M - H]^-$, calculated for $C_{14}H_7O_4N_2Br_2$ $[M - H]^-$: 424.87671.

Dimethyl 6,9-dibromo-7,8-dihydroxyphenazine-2,3-dicarboxylate (4). A solution of bromanilic acid (1.28 g, 4.29 mmol) and **1** (0.961 g, 4.29 mmol) in ethanol (350 mL) was stirred at 80 °C overnight. After the disappearance of the reactants, the reaction mixture was cooled to room temperature, and the precipitate was filtered and washed with a small amount of ethanol to obtain **4** as a red solid (1.59 g, 76% yield); m.p. over 300 °C; IR (ATR): $\tilde{\nu}$ = 3204, 2951, 1701, 1649, 1622, 1611, 1587, 1572, 1557, 1508 cm^{-1}; ^1H NMR (500 MHz, DMSO-d_6): δ = 8.36 (br, 2H, aromatic), 3.89 (s, 6H, CH_3) ppm; the ^{13}C NMR spectrum could not be obtained because of the low solubility in any solvents; HRMS (APCI): m/z found 484.89825 $[M + H]^+$, calculated for $C_{16}H_{11}O_6N_2Br_2$ $[M + H]^+$: 484.89784.

Methyl 6,9-dibromo-7,8-bis(methoxymethoxy)phenazine-2-carboxylate (5). A solution of sodium hydride abt. 60% oil suspension (328 mg, 20 eq.) and **3** (172 mg, 0.404 mmol) in THF (100 mL) was stirred at 0 °C for 30 min. Then, chloromethyl methyl ether (608 μL, 8.08 mmol) was added to the solution, and the mixture was stirred at 0 °C overnight. After concentrating under reduced pressure, the residue was chromatographed on silica gel (ethyl acetate/dichloromethane = 1/3 as an eluent) to obtain **5** as a yellow solid (155 mg, 75% yield); m.p. 160–161 °C; IR (ATR): $\tilde{\nu}$ = 2924, 2839, 1709, 1591 cm^{-1}; ^1H NMR (500 MHz, $CDCl_3$): δ = 9.11 (s, 1H, aromatic), 8.45–8.39 (m, 2H, aromatic), 5.45–5.44 (s, 4H, CH_2), 4.05 (s, 3H, CH_3), 3.75 (s, 6H, CH_3) ppm; the ^{13}C NMR spectrum could not be obtained because of the low stability in $CDCl_3$ and acetone-d_6; HRMS (APCI): m/z found 536.92700 $[M + Na]^+$, calculated for $C_{18}H_{16}O_6N_2Br_2Na$ $[M + Na]^+$: 536.92673.

Dimethyl 6,9-dibromo-7,8-bis(methoxymethoxy)phenazine-2,3-dicarboxylate (6). A solution of sodium hydride abt. 60% oil suspension (307 mg, 15 eq.) and **4** (250 mg, 0.514 mmol) in dry DMF (250 mL) was stirred at 0 °C for 20 min under a N_2 atmosphere. Then, bromomethyl methyl ether (610 μL, 7.71 mmol) was added to the solution, and the mixture was stirred at 0 °C for 90 min. The reaction was quenched with water, and then the solution was extracted with ethyl acetate and hexane (=1/4). After concentrating under reduced pressure, the residue was chromatographed on silica gel (ethyl acetate/dichloromethane = 1/3 as an eluent) to obtain **6** as a yellow solid (123 mg, 42% yield); m.p. 166–168 °C; IR (ATR): $\tilde{\nu}$ = 2953, 1722 cm^{-1}; ^1H NMR (500 MHz, $CDCl_3$): δ = 8.78 (s, 2H, aromatic), 5.46 (s, 4H, CH_2), 4.02 (s, 6H, CH_3), 3.75 (s, 6H, CH_3) ppm; the ^{13}C NMR (125 MHz, $CDCl_3$) δ = 166.96, 153.54, 142.60, 141.08, 133.27, 131.80, 117.03, 100.47, 58.96, 53.25 ppm; HRMS (ESI): m/z found 572.95044 $[M + H]^+$, calculated for $C_{20}H_{19}O_8N_2Br_2$ $[M + H]^+$: 572.95027.

Methyl 7,8-bis(methoxymethoxy)-6,9-bis(5-(4,4,5,5-tetramethyl-1,3-dioxolan-2-yl)thiophen-2-yl)phenazine-2-carboxylate (7). A solution of **5** (235 mg, 0.455 mmol), **2** (567 mg, 1.51 mmol), and $Pd(PPh_3)_4$ (89 mg, 0.0770 mmol) in toluene (110 mL) was stirred at 110 °C for 24 h. After concentrating under reduced pressure, the residue was chromatographed on silica gel (ethyl acetate/hexane = 1/3 as an eluent) to obtain **7** as a red solid (292 mg, 82% yield); m.p. 104–106 °C; IR (ATR): $\tilde{\nu}$ = 2955, 2872, 1726, 1622, 1580, 1537 cm^{-1}; ^1H NMR (500 MHz, $CDCl_3$): δ = 8.87 (s, 1H, aromatic), 8.38 (d, J = 1.90 Hz, 1H, aromatic), 8.30 (d, J = 1.90 Hz, 1H, aromatic), 7.81(d, J = 3.75 Hz, 1H, aromatic), 7.78 (d, J = 3.75 Hz, 1H, aromatic), 7.37–7.20 (m, 2H, aromatic), 6.31 (s, 1H, CH), 6.30 (s, 1H, CH), 5.30 (s, 4H, CH_2), 4.03 (s, 3H, CH_3), 3.30 (s, 6H, CH_3), 1.36–1.33 (m, 24H, CH_3) ppm; ^{13}C NMR (125 MHz, $CDCl_3$): δ = 166.63, 151.96, 151.27, 146.58, 146.50, 143.18, 141.24, 140.96, 140.83, 133.88, 133.85, 133.03, 131.31, 131.28, 131.20, 129.97, 129.09, 125.26, 125.22, 125.05, 124.83, 99.80, 99.76, 97.20, 97.18, 83.28, 83.26, 58.06, 58.05, 52.74, 24.37, 24.34, 22.28, 22.27 ppm; HRMS (ESI): m/z found 801.24866 $[M + Na]^+$, calculated for $C_{40}H_{46}O_{10}N_2NaS_2$ $[M + Na]^+$: 801.24861.

Dimethyl 7,8-bis(methoxymethoxy)-6,9-bis(5-(4,4,5,5-tetramethyl-1,3-dioxolan-2-yl)thiophen-2-yl)phenazine-2,3-dicarboxylate (8). A solution of **6** (55.0 mg, 0.0960 mmol), **2** (144 mg, 0.380 mmol), and $Pd(PPh_3)_4$ (50 mg, 0.0428 mmol) in toluene (50 mL) was stirred at 110 °C for 24 h. After concentrating under reduced pressure, the residue was chromatographed on silica gel (ethyl acetate/dichloromethane = 1/3 as an eluent) to obtain **8** as a red solid (71.0 mg, 89% yield); m.p. 61–63 °C; IR (ATR): $\tilde{\nu}$ = 2978, 1728 cm^{-1}; ^1H NMR (500 MHz, acetone-d_6): δ = 8.56 (s, 2H, aromatic), 7.81–7.75 (m, 2H, aromatic), 7.35–7.29 (m, 2H, aromatic), 6.31 (s, 2H, CH), 5.31 (s, 4H, CH_2), 3.98 (s, 6H, CH_3), 3.30 (s, 6H, CH_3), 1.34 (m, 24H, CH_3) ppm; ^{13}C NMR (125 MHz, acetone-d_6): δ = 167.61, 153.49, 148.20, 142.63, 142.05, 134.31, 133.61, 132.28, 132.21, 126.01, 125.72, 100.77, 97.81, 83.75, 58.18, 53.39, 24.70, 22.53 ppm; HRMS (APCI): m/z

found 837.27246 $[M + H]^+$, calculated for $C_{42}H_{49}O_{12}N_2S_2$ $[M + H]^+$: 837.27214.

7,8-Bis(methoxymethoxy)-6,9-bis(5-(4,4,5,5-tetramethyl-1,3-dioxolan-2-yl)thiophen-2-yl)phenazine-2-carboxylic acid (9). A solution of **9** (106 mg, 0.136 mmol) and NaOH (100 mg) in the mixture of methanol (85 mL), water (17 mL), and THF (10 mL) was stirred at 40 °C for 3 h. After concentrating under reduced pressure, the residue was neutralized with 1 N HCl aq. and extracted into dichloromethane to obtain **9** as a red solid (97 mg, 93% yield); m.p. 211–212 °C; IR (ATR): $\tilde{\nu}$ = 2976, 2926, 2851, 1717, 1699, 1653, 1558, 1541, 1506 cm^{-1}; ^1H NMR (500 MHz, acetone-d_6): δ = 8.91 (dd, J = 1.90 Hz and 0.55 Hz, 1H, aromatic), 8.42 (dd, J = 9.00 Hz and 1.90 Hz, 1H, aromatic), 8.31 (dd, J = 9.00 Hz and 0.61 Hz, 1H, aromatic), 7.82 (d, J = 3.70 Hz, 1H, aromatic), 7.78 (d, J = 3.70 Hz, 1H, aromatic), 7.34–7.27 (m, 2H, aromatic), 6.31 (s, 1H, CH), 6.30 (s, 1H, CH), 5.30 (s, 4H, CH_2), 3.31 (s, 6H, CH_3), 1.38–1.29 (m, 24H, CH_3) ppm; the ^{13}C NMR spectrum could not be obtained because of the low solubility in any solvents; HRMS (ESI): m/z found 765.25153 $[M + H]^+$, calculated for $C_{39}H_{45}O_{10}N_2S_2$ $[M + H]^+$: 765.25101.

7,8-Bis(methoxymethoxy)-6,9-bis(5-(4,4,5,5-tetramethyl-1,3-dioxolan-2-yl)thiophen-2-yl)phenazine-2,3-dicarboxylic acid (10). A solution of **8** (110 mg, mmol) and NaOH (100 mg) in the mixture of methanol (100 mL), water (20 mL), and THF (10 mL) was stirred at 40 °C for 6 h. After concentrating under reduced pressure, the residue was neutralized with 1 N HCl aq. and extracted into dichloromethane to obtain **10** as a red solid (63 mg, 59% yield); m.p. over 300 °C; IR (ATR): $\tilde{\nu}$ = 2976, 2924, 2850, 1728, 1605, 1541, 1508 cm^{-1}; ^1H NMR (500 MHz, acetone-d_6): δ = 9.24 (s, 2H, aromatic), 7.81 (d, J = 3.75 Hz, 2H, aromatic), 7.30 (d, J = 3.70 Hz, 2H, aromatic), 6.30 (s, 2H, CH), 5.29 (s, 4H, CH_2), 3.31 (s, 6H, CH_3), 1.37–1.29 (m, 24H, CH_3) ppm; the ^{13}C NMR spectrum could not be obtained because of the low solubility in any solvents; HRMS (ESI): m/z found 807.22552 $[M - H]^-$, calculated for $C_{40}H_{43}O_{12}N_2S_2$ $[M - H]^-$: 807.22519.

6,9-Bis(5-formylthiophen-2-yl)-7,8-dihydroxyphenazine-2-carboxylic acid (KY-1). A solution of **9** (175 mg) and 1 N HCl aq. (0.5 mL) in the mixture of THF (100 mL) and water (100 mL) was stirred at 70 °C overnight. The precipitate was filtered and washed with hexane to obtain **KY-1** as a black solid (70 mg, 64% yield); m.p. over 300 °C; IR (ATR): $\tilde{\nu}$ = 3505, 3159, 2961, 2799, 2737, 2349, 2085, 1996, 1989, 1703, 1643, 1614, 1557, 1520, 1508 cm^{-1}; ^1H NMR (500 MHz, DMSO-d_6): δ = 9.97 (s, 1H, CHO), 9.93 (s, 1H, CHO), 8.96 (s, 1H, aromatic), 8.76 (d, J = 3,20 Hz, aromatic), 8.71–8.70 (m, 1H, aromatic), 8.19–8.16 (m, 2H, aromatic), 8.04–8.00 (m, 2H, aromatic) ppm; the ^{13}C NMR spectrum could not be obtained because of the low solubility in any solvents; HRMS (APCI): m/z found 477.02100 $[M + H]^+$, calculated for $C_{23}H_{13}O_6N_2S_2$ $[M + H]^+$: 477.02095.

6,9-Bis(5-formylthiophen-2-yl)-7,8-dihydroxyphenazine-2,3-dicarboxylic acid (KY-2). A solution of **10** (63.0 mg, mmol) and 1 N HCl aq. (2 mL) in the mixture of THF (50 mL) and water (50 mL) was stirred at 70 °C overnight. The precipitate was filtered and washed with hexane to obtain **KY-2** as a black solid (8.00 mg, 20% yield); m.p. over 300 °C; IR (ATR): $\tilde{\nu}$ = 3198, 2376, 2347, 2160, 1726, 1701, 1697, 1678, 1655, 1612, 1595, 1535 cm^{-1}; ^1H NMR (500 MHz, DMSO-d_6): δ = 9.95 (s, 2H, CHO), 8.91–8.87 (m, 2H, aromatic), 8.34 (s, 2H, aromatic), 8.01 (d, J = 4.25 Hz, 2H, aromatic) ppm; ^{13}C NMR spectrum could not be obtained because of the low solubility in any solvents; HRMS (ESI): m/z found 518.99603 $[M - H]^-$, calculated for $C_{24}H_{11}O_8N_2S_2$ $[M - H]^-$: 518.99513.

Sodium 6,9-bis(5-formylthiophen-2-yl)-7,8-dihydroxyphenazine-2-carboxylate (KY-1Na). A solution of **KY-1** (42 mg, 0.881 mmol) and 1 N NaOH aq. (70 μL) in water (100 mL) was stirred at room temperature for 10 min and concentrated to obtain **KY-1Na** as a red solid (46% yield); m.p. over 300 °C; IR (ATR): $\tilde{\nu}$ = 3200, 2303, 2110, 1994, 1846, 1578 cm^{-1}; ^1H NMR (500 MHz, D_2O): δ = 9.51 (s, 1H, CHO), 9.36 (s, 1H, CHO), 8.71 (s, 1H, aromatic), 8.59 (s, 1H, aromatic), 8.43 (s, 1H, aromatic), 8.00 (d, J = 8.62 Hz, 1H, aromatic), 7.93 (d, J = 8.50 Hz, 1H, aromatic), 7.84 (s, 1H, aromatic), 7.68 (s, 1H, aromatic) ppm; the ^{13}C NMR spectrum could not be obtained because of the low solubility in any solvents; HRMS (ESI): m/z found 475.00620 $[M - Na]^-$, calculated for $C_{23}H_{11}O_6N_2S_2$ $[M - Na]^-$: 475.00530.

Sodium 6,9-bis(5-formylthiophen-2-yl)-7,8-dihydroxyphenazine-2,3-dicarboxylate (KY-2Na). A solution of **KY-2** (8.00 mg, 0.0154 mmol) and 1 N NaOH aq. (31.0 μL) in water (50 mL) was stirred at room temperature for 10 min and concentrated to obtain **KY-2Na** as a red solid (10 mg, quant.); m.p. over 300 °C; IR (ATR): $\tilde{\nu}$ = 3318, 1560 cm^{-1}; ^1H NMR (500 MHz, D_2O): δ = 9.84 (s, 1H, CHO), 9.78 (s, 1H, CHO), 8.45 (m, 1H, aromatic), 8.39 (m, 1H, aromatic), 8.27 (s, 1H, aromatic), 8.14 (s, 1H, aromatic), 8.03 (s, 2H, aromatic) ppm; the ^{13}C NMR spectrum could not be obtained because of the low solubility in any solvents; HRMS (APCI): m/z found 518.99615 $[M + H - 2Na]^-$, calculated for $C_{24}H_{11}O_8N_2S_2$ $[M + H - 2Na]^-$: 518.99513.

n-Octanol/water partition coefficient

The log $P_{o/w}$ values were determined from the concentration of PSs partitioned into water (100 mL) and *n*-octanol (100 mL) and the concentration of PSs partitioned into each phase.

Evaluation of the $^1O_2$ quantum yield

$^1O_2$ generation by phenazine-2,3-diol-based PSs **KO-2**, **KY-1**, **KY-2**, **KY-1Na**, and **KY-2Na** was investigated by monitoring the changes in the photoabsorption spectra of DPBF in the DMSO solution of each PS and ABDA in aqueous solution (D_2O/DMSO 99 : 1, v/v) of **KY-1Na** and **KY-2Na** under photoirradiation. DMSO and water were bubbled with air for 15 min prior to preparing solutions. Air-saturated DMSO containing DPBF or aqueous solutions containing ABDA and each PS were irradiated with monochromatic light at 532 nm (300 μW cm^{-2}) that was obtained by passage of a xenon light source (HAL-320, Asahi Spectra) through a monochromator (CMS-100, Asahi Spectra). The concentration of DPBF and ABDA was 5×10^{-5} M in air-saturated DMSO or aqueous solutions. The concentration of the PSs and **RB** was adjusted so that the absorbance was *ca.* 0.03 at an irradiation wavelength of 532 nm.

Except for nonirradiated solutions, each spectrum was measured immediately after photoirradiation for 1 min. The procedure using DPBF and ABDA was promptly repeated until the total photoirradiation time reached 10 min and 60 min, respectively. The changes in the optical density (ΔOD) of DPBF and ABDA were plotted against the photoirradiation time to obtain the slopes (m). The Φ_Δ values of **KO-2**, **KY-1**, **KY-2**, **KY-1Na**, and **KY-2Na** were determined using the relative method using **RB** (Φ_Δ = 0.76 in DMSO[9a] and 0.75 in water[9b]) as a standard according to the following equation:

$$\Phi_{\Delta\mathrm{sam}} = \Phi_{\Delta\mathrm{ref}} \times [(m_{\mathrm{sam}}/m_{\mathrm{ref}}) \times (L_{\mathrm{ref}}/L_{\mathrm{sam}})]$$

where $\Phi_{\Delta\mathrm{sam}}$ and $\Phi_{\Delta\mathrm{ref}}$ are the $^1O_2$ quantum yields of phenazine-2,3-diol-based PSs and **RB**, respectively, m_{sam} and m_{ref} are slopes in the plots of ΔOD at the photoabsorption maximum wavelength of DPBF (415 nm) or ABDA (400 nm) against the photoirradiation time, and L_{sam} and L_{ref} are light harvesting efficiencies, which are given by L = $1–10^{-A}$ ("A" is the absorbance at the photoirradiation wavelength).

Evaluation of the cellular uptake of KY-2Na

Colon26 cells were seeded on glass bottom dishes at a density of 1×10^5 cells per well and incubated overnight. The cells were treated with **KY-2Na** for 24 h. The medium was collected and the fluorescence spectrum was recorded. Then, the cells were observed under a confocal laser scanning microscope (LSM700, Carl Zeiss, Germany).

Photodynamic activity against cancer cell lines

Colon26 cells were seeded on 48-well plates (Thermo Fischer Science) at 1.71×10^4 cells (N = 3) and incubated overnight (approximately 18 h). The cells were exposed to **KY-1Na** or **KY-2Na** at varying concentrations. After 24 h of incubation, the cells were washed with PBS thrice, and photoirradiation (>510 nm, 9 mW cm^{-2}) was carried out for 30 min. Afterward, the cells were incubated for 24 h, and the Cell Counting Kit-8 solution was added to the cells. After 30 min of incubation, the absorbance at 450 nm was measured using a microplate reader.

Theoretical calculations

The Gaussian 16 program[21] was used for density functional theory (DFT) calculations and time-dependent DFT (TD-DFT) calculations. DFT and TD-DFT calculations at the B3LYP/6-311G(d,p)/DMSO-IEFPCM level for **KO-2**, **KY-1**, and **KY-2**, the B3LYP/6-311+G(d,p)/DMSO-IEFPCM level for **KY-1Na** and **KY-2Na** in carboxylate anion forms, and the B3LYP/6-311+G(d,p)/Water-IEFPCM level for **KY-1Na** and **KY-2Na** in carboxylate anion forms were performed. Geometrical optimizations of the S_0 state at each calculation level were performed with frequency calculations. There are no imaginary frequencies for all optimized structures. The TD-DFT calculations of both excited singlet and triplet states were performed using optimized S_0 geometries.

Conflicts of interest

There are no conflicts to declare.

Acknowledgements

This work was supported by Grants-in-Aid for Scientific Research (B) from the Japan Society for the Promotion of Science (JSPS) KAKENHI Grant Number 22H02123 and by The Futaba Foundation.

References

1 I. Pibiri, S. Buscemi, A. P. Piccionello and A. Pace, *ChemPhotoChem*, 2018, **2**, 535–547.
2 A. A. Ghogare and A. Greer, *Chem. Rev.*, 2016, **116**, 9994–10034.
3 (*a*) L.-X. Li, L. Min, T.-B. Yao, S.-X. Ji, C. Qiao, P.-L. Tian, J. Sun and C.-C. Li, *J. Am. Chem. Soc.*, 2022, **144**, 18823–18828; (*b*) P. Bayer, J. Schachtner, M. Májek and A. J. von Wangelin, *Org. Chem. Front.*, 2019, **6**, 2877–2883; (*c*) M. Prein and W. Adam, *Angew. Chem., Int. Ed. Engl.*, 1996, **35**, 471–494; (*d*) W. Adam, S. G. Bosio, N. J. Turro and B. T. Wolff, *J. Org. Chem.*, 2004, **69**, 1704–1715; (*e*) A. Greer, *Acc. Chem. Res.*, 2006, **39**, 797–804; (*f*) M. N. Alberti and M. Orfanopoulos, *Chem. – Eur. J.*, 2010, **16**, 9414–9421.
4 (*a*) L. Burchill and J. H. George, *J. Org. Chem.*, 2020, **85**, 2260–2265; (*b*) M. Jaramillo, J. A. Joens and K. E. O'Shea, *Environ. Sci. Technol.*, 2020, **54**, 6073–6081; (*c*) W. Adam, S. G. Bosio and N. J. Turro, *J. Am. Chem. Soc.*, 2002, **124**, 8814–8815; (*d*) W. Adam, C. R. Saha-Möller and S. B. Schambony, *J. Am. Chem. Soc.*, 1999, **121**, 1834–1838.
5 (*a*) M. Gemki, Ö. Taspinar, A. Adler, A. G. Griesbeck, D. Gründemann and H.-G. Schmalz, *Org. Process Res. Dev.*, 2021, **25**, 2747–2753; (*b*) M. Klaper and T. Linker, *Chem. – Eur. J.*, 2015, **21**, 8569–8577; (*c*) W. Adam and M. Prein, *Acc. Chem. Res.*, 1996, **29**, 275–283; (*d*) C. S. Foote, *Acc. Chem. Res.*, 1968, **1**, 104–110.
6 (*a*) D. Garcia-Fresnadillo, *ChemPhotoChem*, 2018, **2**, 512–534; (*b*) M. L. Marin, L. Santos-Juanes, A. Arques, A. M. Amat and M. A. Miranda, *Chem. Rev.*, 2012, **112**, 1710–1750; (*c*) E. Díez-Mato, F. C. Cortezón-Tamarit, S. Bogialli, D. García-Fresnadillo and M. D. Marazuela, *Appl. Catal., B*, 2014, **160–161**, 445–455; (*d*) H. Kim, W. Kim, Y. Mackeyev, G. S. Lee, H. J. Kim, T. Tachikawa, S. Hong, S. Lee, J. Kim, L. J. Wilson, T. Majima, P. J. Alvarez, W. Choi and J. Lee, *Environ. Sci. Technol.*, 2012, **46**, 9606–9613.
7 (*a*) F. Manjón, M. Santana-Magaña, D. García-Fresnadillo and G. Orellana, *Photochem. Photobiol. Sci.*, 2014, **13**, 397–406; (*b*) F. Manjón, M. Santana-Magaña, D. García-Fresnadillo and G. Orellana, *Photochem. Photobiol. Sci.*, 2010, **9**, 838–845; (*c*) F. Manjón, D. García-Fresnadillo and G. Orellana, *Photochem. Photobiol. Sci.*, 2009, **8**, 926–932;

(*d*) L. Villén, F. Manjón, D. García-Fresnadillo and G. Orellana, *Appl. Catal., B*, 2006, **69**, 1–9; (*e*) F. Manjón, L. Villén, D. García-Fresnadillo and G. Orellana, *Environ. Sci. Technol.*, 2008, **42**, 301–307.

8 (*a*) L. Benov, *Med. Princ. Pract.*, 2015, **24**, 14–28; (*b*) G. Gunaydin, E. M. Gedik and S. Ayan, *Front. Chem.*, 2021, **9**, 691697; (*c*) A. Kamkaew, S. H. Lim, H. B. Lee, L. V. Kiew, L. Y. Chung and K. Burgess, *Chem. Soc. Rev.*, 2013, **42**, 77–88.

9 (*a*) R. W. Redmond and J. N. Gamlin, *Photochem. Photobiol.*, 1999, **70**, 391–475; (*b*) L. V. Lutkus, S. S. Rickenbach and T. M. McCormick, *J. Photochem. Photobiol., A*, 2019, **378**, 131–135; (*c*) A. Gollmer, A. Felgenträger, W. Bäumler, T. Maisch and A. Späth, *Photochem. Photobiol. Sci.*, 2015, **14**, 335–351; (*d*) I. Walker, S. A. Gorman, R. D. Cox, D. I. Vernon, J. Griffiths and S. B. Brown, *Photochem. Photobiol. Sci.*, 2004, **3**, 653–659; (*e*) S. A. Gorman, A. L. Bell, J. Griffiths, D. Roberts and S. B. Brown, *Dyes Pigm.*, 2006, **71**, 153–160; (*f*) C. Li, Y. Huang, K. Lai, B. A. Rasco and Y. Fan, *Food Control*, 2016, **65**, 99–105; (*g*) S. Soltanian, A. Gholamhosseini and M. Banaee, *Aquacult. Res.*, 2021, **52**, 2640–2650.

10 (*a*) J. Varchola, K. Želonková, D. Chorvat Jr., D. Jancura, P. Miskovsky and G. Bánó, *J. Lumin.*, 2016, **177**, 17–21; (*b*) X. T. Zheng, Y. C. Lai and Y. N. Tan, *Nanoscale Adv.*, 2018, **1**, 2250–2257; (*c*) H.-J. Chen, X.-B. Zhou, A.-L. Wang, B.-Y. Zheng, C.-K. Yeh and J.-D. Huang, *Eur. J. Med. Chem.*, 2018, **145**, 86–95.

11 (*a*) R. Bücher, V. V. da Cruz, N. Brover, A. Charisiadis, M. Fondell, R. Haverkamp, M. O. Senge and A. Föhlisch, *Phys. Chem. Chem. Phys.*, 2022, **24**, 7505–7511; (*b*) P. G. Mahajan, N. C. Dige, B. D. Vanjare, A. R. Phull, S. J. Kim, S.-K. Hong and K. H. Lee, *J. Fluoresc.*, 2018, **28**, 871–882; (*c*) D. T. Payne, J. Hynek, J. Labuta and J. P. Hill, *Phys. Chem. Chem. Phys.*, 2022, **24**, 6146–6154; (*d*) P. M. Antoni, A. Naik, I. Albert, R. Rubbiani, S. Gupta, P. Ruiz-Sanchez, P. Munikorn, J. M. Mateos, V. Luginbuehl, P. Thamyongkit, U. Ziegler, G. Gasser, G. Jeschke and B. Spingler, *Chem. – Eur. J.*, 2015, **21**, 1179–1183.

12 O. J. Stacey and S. J. A. Pope, *RSC Adv.*, 2013, **3**, 25550–25564.

13 (*a*) J. Miao, Y. Huo, G. Yao, Y. Feng, J. Weng, W. Zhao and W. Guo, *Angew. Chem., Int. Ed.*, 2022, **61**, e202201815; (*b*) L. A. Ortiz-Rodriguez, S. J. Hoehn, A. Loredo, L. Wang, H. Xiao and C. E. Crespo-Hernández, *J. Am. Chem. Soc.*, 2021, **143**(7), 2676–2681.

14 (*a*) K. Ohira, K. Imato and Y. Ooyama, *Mater. Chem. Front.*, 2021, **5**, 5298–5304; (*b*) K. Imato, K. Ohira, M. Yamaguchi, T. Enoki and Y. Ooyama, *Mater. Chem. Front.*, 2020, **4**, 589–596.

15 S. Tsumura, K. Ohira, K. Hashimoto, K. Imato and Y. Ooyama, *Mater. Chem. Front.*, 2020, **4**, 2762–2771.

16 M. Li, B. Dyett and X. Zhang, *Anal. Chem.*, 2019, **91**, 10371–10375.

17 H.-B. Guo, F. He, B. Gu, L. Liang and J. C. Smith, *J. Phys. Chem. A*, 2012, **116**, 11870–11879.

18 (*a*) K. Golinick and A. Griesbeck, *Tetrahedron*, 1985, **41**, 2057–2068; (*b*) D. Steinebrunner, G. Schnurpfeil, H. H. Doebler, J. A. T. Burgos, D. Wöhrle and A. Wittstock, *Photochem. Photobiol. Sci.*, 2021, **20**, 547–558; (*c*) T. Entradas, S. Waldron and M. Volk, *J. Photochem. Photobiol., B*, 2020, **204**, 111787.

19 R. Kawasaki, K. Yamana, R. Shimada, K. Sugikawa and A. Ikeda, *ACS Omega*, 2021, **6**, 3209–3217.

20 N. J. Yang and M. J. Hinner, *Methods Mol. Biol.*, 2015, **1266**, 29–53.

21 M. J. Frisch, G. W. Trucks, H. B. Schlegel, G. E. Scuseria, M. A. Robb, J. R. Cheeseman, G. Scalmani, V. Barone, G. A. Petersson, H. Nakatsuji, X. Li, M. Caricato, A. V. Marenich, J. Bloino, B. G. Janesko, R. Gomperts, B. Mennucci, H. P. Hratchian, J. V. Ortiz, A. F. Izmaylov, J. L. Sonnenberg, D. Williams-Young, F. Ding, F. Lipparini, F. Egidi, J. Goings, B. Peng, A. Petrone, T. Henderson, D. Ranasinghe, V. G. Zakrzewski, J. Gao, N. Rega, G. Zheng, W. Liang, M. Hada, M. Ehara, K. Toyota, R. Fukuda, J. Hasegawa, M. Ishida, T. Nakajima, Y. Honda, O. Kitao, H. Nakai, T. Vreven, K. Throssell, J. A. Montgomery Jr., J. E. Peralta, F. Ogliaro, M. J. Bearpark, J. J. Heyd, E. N. Brothers, K. N. Kudin, V. N. Staroverov, T. A. Keith, R. Kobayashi, J. Normand, K. Raghavachari, A. P. Rendell, J. C. Burant, S. S. Iyengar, J. Tomasi, M. Cossi, J. M. Millam, M. Klene, C. Adamo, R. Cammi, J. W. Ochterski, R. L. Martin, K. Morokuma, O. Farkas, J. B. Foresman and D. J. Fox, *Gaussian 16, Revision B.01*, Gaussian, Inc., Wallingford, CT, 2016.

22 H. Uoyama, K. Goushi, K. Shizu, H. Nomura and C. Adachi, *Nature*, 2012, **492**, 234–238.

23 F. Hu, S. Xu and B. Liu, *Adv. Mater.*, 2018, **30**, 1801350.

